Structural, Magnetic, and Ion-Exchange Properties of $RbMnHP_3O_{10}$

A. J. Wright and J. P. Attfield*,†

Department of Chemistry, University of Cambridge, Lensfield Road, Cambridge CB2 1EW, U.K.

Received February 26, 1998

The crystal structure, magnetic properties, and ion-exchange behavior of $RbMnHP_3O_{10}$ have been determined. The crystal structure ($a = 12.1866(3)$ Å, $b = 8.3586(2)$ Å, $c = 9.0763(3)$ Å, $\beta = 109.067(1)°$, space group $C2/c$), determined from X-ray powder diffraction, is of $NH_4FeHP_3O_{10}$ type, consisting of hydrogen triphosphate anions linking Jahn−Teller distorted $Mn^{III}O_6$ octahedra around Rb^+ cations. Magnetic susceptibility measurements and low-temperature neutron powder diffraction show that $RbMnHP_3O_{10}$ behaves as a Curie−Weiss paramagnet at high temperatures and orders antiferromagnetically below a Néel temperature of 10 K. The magnetic structure is commensurate with the nuclear cell, and the collinear antiferromagnetic structure has magnetic symmetry group P_C2/c' with spins of 3.82(6) μ_B lying in the *ac* plane. Exchange of H^+ for Li^+ has not proved possible without a breakdown of the $RbMnHP_3O_{10}$ framework due to strong symmetric hydrogen bonding between triphosphate anions.

Introduction

The properties of inorganic framework materials are of importance in many areas of current research. This can be attributed to both the relevance of their chemical behavior and their diversity. Some have the ability to catalyze organic reactions within their frameworks,[1] while others exhibit enhanced ion-exchange properties or high ionic conductivity[2,3] which find applications in rechargeable batteries and fuel cells research. Such properties are mainly a consequence of the open framework structures adopted by these materials and have led to an intensive worldwide search for materials with similar structural characteristics. This has produced numerous new examples, among which are transition metal phosphate frameworks such as FePO's,[4] ZnPO's,[5] and CoPO's.[6] The magnetic properties of many of these materials are also of fundamental interest in understanding the nature of magnetic interactions.

We are currently searching for new framework materials with the ability to "switch" between distinct framework geometries by means of ion exchange, leading to the possibility of flexible host materials. This behavior, first demonstrated by Li^+/H^+ exchange in $MnAsO_4{\cdot}H_2O$,[7] requires the presence of Jahn−Teller cations in the framework. The exchange of Li^+ for H^+ produces a switch in the framework geometry, resulting from cooperative changes to the Jahn−Teller distortions of the MnO_6 octahedra. This has led us to study the series of phases, $AMnHP_3O_{10}$ (A = K, Rb, Cs) which contain high-spin $3d^4$ Mn^{3+}. The structure of $CsMnHP_3O_{10}$ has previously been reported[8] from a single-crystal X-ray diffraction study and is known to consist of chains of HP_3O_{10} units, interlinked by tetragonally distorted MnO_6 octahedra, to form a three-dimensional framework. $RbMnHP_3O_{10}$ was first prepared by Guzeeva and Tananaev,[9] who reported an X-ray powder diffraction pattern but no further crystallographic information. Here we report the crystal structure and magnetic properties of this phase and some attempts to exchange the H^+ ion by Li^+.

Experimental Section

$RbMnHP_3O_{10}$ was prepared from a solution of Rb_2CO_3, Mn_2O_3, H_3PO_4 (85%), and concentrated HNO_3 in a molar ratio of Rb:Mn:P:N of 7:2:20:5. This solution was heated to 250 °C for 48 h and then slowly cooled to room temperature over 12 h, after which the brown microcrystalline product was collected by filtration and washed with water. The nitric acid in the reaction mixture maintains the Mn^{3+} oxidation state during the reaction.

The X-ray powder diffraction pattern of the product matched that reported for $RbMnHP_3O_{10}$,[9] and a long scan ($2\theta = 4-100°$, 0.02° steps, 10 s per step) was performed for structure determination on a Phillips PW1710 diffractometer using unmonochromated Cu Kα radiation. Neutron powder diffraction data were collected on the D20 instrument at ILL, Grenoble, France. This instrument contains 1600 detectors positioned in 0.1° intervals in the range 0−160° in 2θ. Data were collected at a wavelength of 2.4177 Å for 30 min. Rietveld analyses[10] of the X-ray and neutron data were performed using the GSAS software package[11] to refine the crystal and magnetic structures for this material.

Magnetic susceptibility data were collected on a 57.8 mg sample of $RbMnHP_3O_{10}$ from 4 to 100 K in a field of 1 T on a Quantum Design SQUID magnetometer. The sample had previously been cooled in zero field.

Ion exchange of H^+ for Li^+ was attempted using a number of methods. These included a solid-state reaction of intimately mixed $RbMnHP_3O_{10}$ and a lithium salt ($LiNO_3$ or Li_2CO_3 or LiOH or LiCl) in molar ratios varying from 1:1 to 1:10 at temperatures ranging from

† E-mail: jpa14@cam.ac.uk. Fax: +44 1223 336362.

(1) Thomas, J. M. *Angew. Chem., Int. Ed. Engl.* **1994**, *33*, 913−937.
(2) Brochu, R.; Lamzibri, A.; Aadane, A.; Arsalane, S.; Ziyad, M. *Eur. J. Solid State Inorg. Chem.* **1991**, *28*, 253−270.
(3) Clearfield, A. *Eur. J. Solid State Inorg. Chem.* **1991**, *28*, 37−56.
(4) Corbin, D. R.; Whitney, J. F.; Fultz, W. C.; Stucky, G. D.; Eddy, M. M.; Cheetham, A. K. *Inorg. Chem.* **1986**, *25*, 2279−2280.
(5) Harrison, W. T. A.; Nenoff, T. M.; Eddy, M. M.; Martin, T. E.; Stucky, G. D. *J. Mater. Chem.* **1992**, *2*, 1127−1134.
(6) Chen, J.; Jones, R. H.; Natarajan, S.; Hursthouse, M. B.; Thomas, J. M. *Angew. Chem., Int. Ed. Engl.* **1994**, *33*, 639−640.
(7) Aranda, M. A. G.; Attfield, J. P.; Bruque, S. *J. Chem. Soc., Chem. Commun.* **1991**, 604−606.
(8) Murashova, E. V.; Chudinova, N. N. *Kristallografiya* **1995**, *40*, 476−484.
(9) Guzeeva, L. S.; Tananaev, I. V. *Inorg. Mater.* **1988**, *24*, 538−542.
(10) Rietveld, H. M. *J. Appl. Crystallogr.* **1969**, *2*, 65−71.
(11) Larson, A. C.; Von Dreele, R. B. Los Alamos National Laboratory Report No. LA-UR-86-748, 1994.

S0020-1669(98)00212-2 CCC: $15.00
Published on Web 07/10/1998

Table 1. Structural Parameters for $RbMnHP_3O_{10}$ Obtained from Rietveld Analysis of 300 K Powder X-ray Diffraction (Upper Values with Bond Valence Sums[17]) and 2 K Neutron Diffraction Data (Italicized Lower Values Where Different) in Space Group *C2/c*, with Esd's in Parentheses

Fitting Factors

$R_{wp} = 3.0\%$	$R_p = 2.2\%$	$R_F^2 = 7.0\%$	$\chi^2 = 5.2$
2.5%	*1.8%*	*3.6%*[a]	*4.4*

Lattice Parameters

$a = 12.1866(3)$ Å	$b = 8.3586(2)$ Å	$c = 9.0763(3)$ Å	$\beta = 109.067(1)°$
12.178(1) Å	*8.3513(9) Å*	*9.089(1) Å*	*108.990(5)°*

Positional Parameters

atom	site	*x*	*y*	*z*	U_{iso}/Å^2 [b]	BVS
Rb	4e	0	0.4358(3)	1/4	0.047(2)	0.95
			0.437(1)		*0.033(4)*	
Mn	4c	1/4	1/4	0	0.011(2)	2.99
					0.001(1)	
P(1)	8f	0.2922(4)	0.5590(5)	0.2060(4)	0.001(1)	5.48
		0.2907(8)	*0.563(1)*	*0.207(1)*	*0.001*	
P(2)	4f	1/2	0.3681(7)	1/4	0.001	5.22
			0.368(1)		*0.001*	
O(1)	8f	0.4181(6)	0.4854(7)	0.2973(8)	0.003(2)	2.20
		0.4157(7)	*0.485(1)*	*0.303(1)*	*0.001*	
O(2)	8f	0.2213(6)	0.4335(9)	0.1093(7)	0.003	2.27
		0.2147(7)	*0.430(1)*	*0.102(1)*	*0.001*	
O(3)	8f	0.3272(6)	0.6980(8)	0.1247(7)	0.003	1.87
		0.3235(7)	*0.707(1)*	*0.115(1)*	*0.001*	
O(4)	8f	0.2431(6)	0.6039(9)	0.3252(7)	0.003	2.23
		0.2401(7)	*0.617(1)*	*0.324(1)*	*0.001*	
O(5)	8f	0.4400(7)	0.2753(7)	0.1069(7)	0.003	1.73
		0.4341(6)	*0.281(1)*	*0.114(1)*	*0.001*	
H	4d	1/4	1/4	1/2	0.003	0.67
					0.032(8)	

[a] R_F^2 values for the nuclear and magnetic reflections were 3.3% and 14.1%. [b] Values shown without esd's were constrained to be equal to those of the atom above.

150 to 250 °C, for up to 4 weeks. Refluxing $RbMnHP_3O_{10}$ with LiCl in 1-hexanol at 150 °C was also attempted. In those cases when a reaction occurred, a mixture of phases was formed including Li_3PO_4 which indicated that the framework structure had been broken down. No evidence for a Li-exchanged product was observed.

Results

Crystal Structure. The X-ray powder pattern obtained from $RbMnHP_3O_{10}$ clearly indicated a structure type different from that of $CsMnHP_3O_{10}$.[8] The pattern was indexed from 22 accurately measured reflection positions using the Treor program[12] on a *C*-centered monoclinic cell ($a = 12.180(1)$ Å, $b = 8.355(1)$ Å, $c = 9.075(1)$ Å, $\beta = 109.07(1)°$). This cell is similar to that of $NH_4FeHP_3O_{10}$,[13] which has *C*2/*c* space group symmetry, and so this structure was used as the initial model for the Rietveld analysis. The refinement, which utilized an asymmetry corrected pseudo-Voigt peak shape,[14,15] a linear interpolated background function, and a surface roughness correction,[16] converged to $R_{wp} = 3.0\%$. The final refined structural parameters are listed in Table 1, with bond lengths and angles shown in Table 2. The fitted profile is displayed in Figure 1, and views of the structure are shown in Figures 2 and 3. Bond valence sum (BVS) calculations were performed using the method and parameters of Brown and Altermatt,[17] and these are also listed in Table 1.

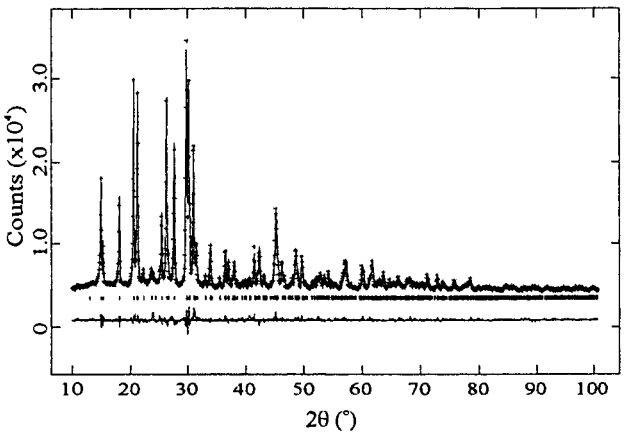

Figure 1. Observed (+), calculated, and difference X-ray powder diffraction profiles of $RbMnHP_3O_{10}$ at 300 K.

Table 2. Bond Lengths (Å) and Selected Angles (deg) for $RbMnHP_3O_{10}$ Obtained from Rietveld Analysis of 300 K X-ray Powder Diffraction Data, with Esd's in Parentheses

Mn−O(2)	1.919(8) (×2)	O(2)−Mn−O(2′)	180
Mn−O(4)	1.982(8) (×2)	O(2)−Mn−O(4)	87.4(3)
Mn−O(5)	2.209(7) (×2)	O(2)−Mn−O(4′)	92.6(3)
		O(2)−Mn−O(5)	92.2(3)
P(1)−O(1)	1.609(6)	O(2)−Mn−O(5′)	87.8(3)
P(1)−O(2)	1.458(8)	O(4)−Mn−O(4′)	180
P(1)−O(3)	1.510(7)	O(4)−Mn−O(5)	93.3(3)
P(1)−O(4)	1.446(7)	O(4)−Mn−O(5′)	86.8(3)
P(2)−O(1)	1.556(6) (×2)		
P(2)−O(5)	1.484(6) (×2)	O(1)−P(1)−O(2)	108.2(5)
		O(1)−P(1)−O(3)	99.9(4)
Rb−O(2)	3.340(6) (×2)	O(2)−P(1)−O(3)	117.8(5)
Rb−O(2′)	3.654(7) (×2)	O(1)−P(2)−O(1′)	101.9(5)
Rb−O(3)	2.848(7) (×2)	O(1)−P(2)−O(5)	113.2(4)
Rb−O(4)	3.146(7) (×2)	O(1)−P(2)−O(5′)	105.3(4)
Rb−O(5)	3.107(6) (×2)	O(5)−P(2)−O(5′)	117.0(7)
H−O(3)	1.289(6) (×2)	O(3)−H−O(3′)	180
O(3)···O(3′)	2.578(12)		

The Rietveld analysis of the 2 K neutron diffraction data was also achieved with an asymmetry-corrected pseudo-Voigt peak shape[14,18] and a linear interpolated background function. The final refined parameters (from a fit to the nuclear and magnetic intensities as described below) are included in Table 1, and the profile is shown in Figure 4. Although the resolution of the D20 instrument at high 2θ angles limits the accuracy of the refined parameters to below that of the X-ray study, the refinement confirms that the structure type for $RbMnHP_3O_{10}$ at 2 K is the same as that at 300 K, without evidence for any low-temperature structural distortions. Refining the H atom off the high symmetry (1/4, 1/4, 1/2) site did not lead to a significant improvement in the fit, and so H was kept at this position in the final neutron and X-ray refinements.

Magnetic Properties. The magnetic susceptibility data (Figure 5) show that $RbMnHP_3O_{10}$ orders antiferromagnetically with $T_N = 10$ K. At higher temperatures it behaves as a Curie−Weiss paramagnet. The fitted Curie−Weiss curve (after diamagnetic correction) for $RbMnHP_3O_{10}$ gives a Weiss constant $\Theta = -1.2$ K and an effective magnetic moment $\mu_{eff} = 4.6\ \mu_B$ (compared to 4.9 μ_B expected for high-spin $3d^4$ Mn^{3+}).

After the nuclear contribution was fitted for the 2 K neutron diffraction pattern, several magnetic peaks were evident (*see*

(12) Werner, P. E. *Z. Kristallogr.* **1969**, *120*, 375−387.
(13) Krasnikov, V. V.; Konstant, Z. A.; Fundamenskii, V. S. *Inorg. Mater.* **1983**, *19*, 1231−1235.
(14) Thompson, P.; Cox, D. E.; Hastings, J. B. *J. Appl. Crystallogr.* **1987**, *20*, 79−83.
(15) Finger, L. W.; Cox, D. E.; Jephcoat, A. P. *J. Appl. Crystallogr.* **1994**, *27*, 892−900.
(16) Collazo, J.; Hermann, H.; Pitschke, W.; Wetzig, K. *J. Appl. Crystallogr.* **1997**, *30*, 312−319.
(17) Brown, I. D.; Altermatt, D. *Acta Crystallogr.* **1985**, *B41*, 244−247.
(18) Howard, C. J. *J. Appl. Crystallogr.* **1982**, *15*, 615−620.

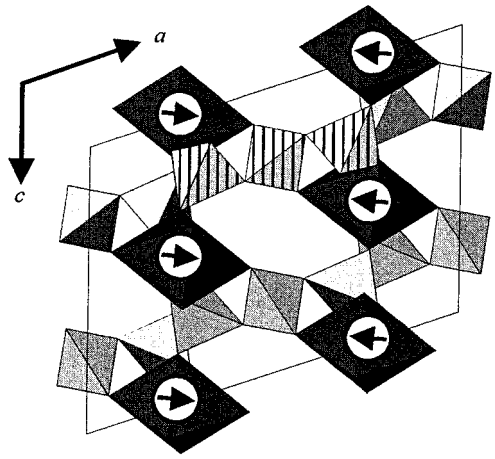

Figure 2. [010] projection of the crystal and magnetic structures of $RbMnHP_3O_{10}$ showing the unit cell. Only the MnO_6 and PO_4 polyhedra are shown, and one P_3O_{10} unit is hatched.

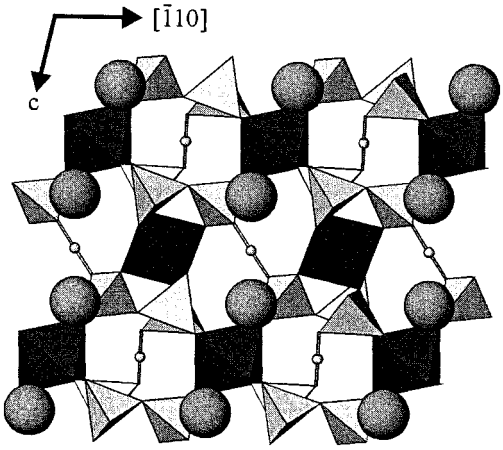

Figure 3. Polyhedral view of the structure of $RbMnHP_3O_{10}$ showing Rb (large spheres) and H atoms (small spheres) enclosed in channels. The symmetric O(3)−H−O(3′) hydrogen bonds are also displayed.

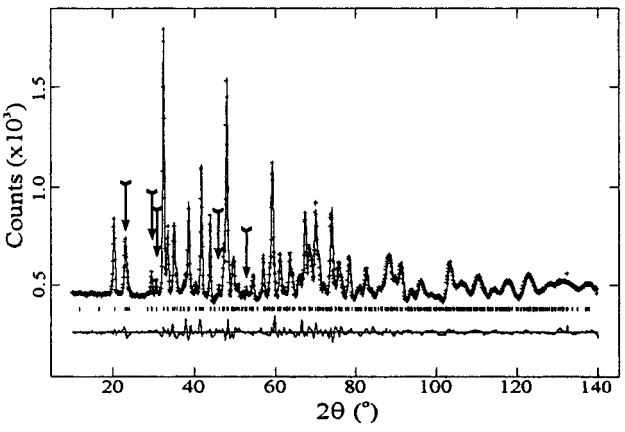

Figure 4. Observed (+), calculated, and difference neutron powder diffraction profiles of $RbMnHP_3O_{10}$ at 2 K. The five magnetic peaks marked in order of increasing 2θ are (011), (210)/(21$\bar{1}$), (10$\bar{2}$), (12$\bar{2}$), and (013).

Figure 4) and were indexed on the same unit cell as the nuclear structure, with reflection conditions consistent with magnetic symmetry group P_C2/c'. The magnetic intensities were Rietveld-fitted using a calculated form factor.[19] Good agreement between observed and calculated intensities was obtained only with the moments in the *ac* plane. Refining the two components gave a resultant moment of 3.82(6) μ_B directed 24(2)° from *a* and 85(2)° from *c*. The relative direction of the four Mn spins in the unit cell are ($^1/_4$, $^1/_4$, 0)+, ($^3/_4$, $^3/_4$, 0)−, ($^3/_4$, $^1/_4$, $^1/_2$)−, and ($^1/_4$, $^3/_4$, $^1/_2$)+, as shown in Figure 2.

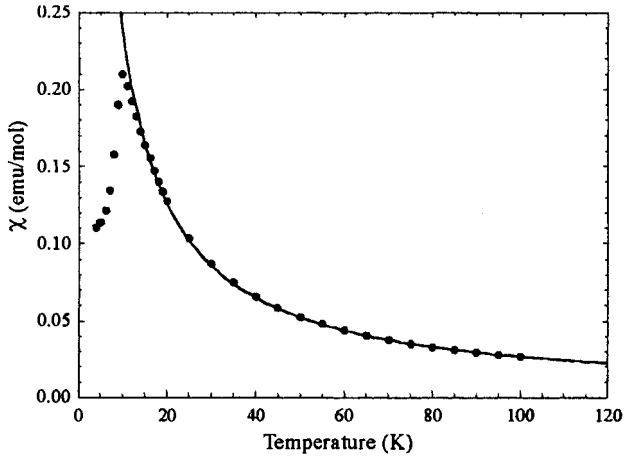

Figure 5. Magnetic susceptibility data for $RbMnHP_3O_{10}$ between 4 and 100 K. The fitted Curie−Weiss curve is also shown.

Discussion

Overall, the structure of $RbMnHP_3O_{10}$, like that of $CsMnHP_3O_{10}$, consists of MnO_6 octahedra linked by hydrogen triphosphate anions around alkali-metal cations. These three-dimensional framework structures can be contrasted to those of other $M^IM^{III}HP_3O_{10}$ materials, such as $NH_4AlHP_3O_{10}$[20] and $CsGaHP_3O_{10}$,[21] which have the M^I cations separating layers of $HP_3O_{10}^{4-}$ and $M^{III}O_6$ units.

The BVS values (Table 1) are in agreement with the expected values, although the bond distances (Table 2) show that the MnO_6 and PO_4 polyhedra are highly distorted. The MnO_6 octahedra show a typical [4 + 2] Jahn−Teller distortion, with four short Mn−O bonds (2 × 1.919(8) Å, 2 × 1.982(8) Å) and two long bonds (2 × 2.209(7) Å). The triphosphate group contains three distorted PO_4 tetrahedra, with long P−O bonds to the bridging O(1) atom, intermediate P(1)−O(3)H distances, and short bonds to the terminal O(2), O(4) and O(5) atoms. This pattern of P−O bond lengths within a P_3O_{10} unit has been observed previously for $CsMnHP_3O_{10}$.[8] Rb^+ is in 10-fold coordination as is Cs^+ in $CsMnHP_3O_{10}$, but the difference in size between these two cations leads to different structures being adopted.

Strong, symmetric O···H···O hydrogen bonding, which is found in many hydrogen phosphates,[22] links the triphosphate anions into chains. The H atom is located at a center of symmetry between two O(3) atoms, but the high thermal factor in the 2 K neutron refinement, equivalent to a root-mean-square displacement of 0.18 Å, suggests that a static or dynamic disorder of H occurs around the mean position. This is consistent with the low BVS value for H^+ as the calculated valence is related exponentially to the bond length. Similar symmetric O···H···O hydrogen bonding found in $CaHPO_4$ at room temperature[23] has been reported to order into long and

(19) Freeman, A. J.; Watson, R. E. *Acta Crystallogr.* **1961**, *14*, 231−234.
(20) Averbuch-Pouchot, M. T.; Durif, A.; Guitel, J. C. *Acta Crystallogr.* **1977**, *B33*, 1436−1438.
(21) Anisimova, N.; Bork, M.; Hoppe, R.; Meisel, M. *Z. Anorg. Allg. Chem.* **1995**, *621*, 1069−1074.
(22) Emsley, J. *Chem. Soc. Rev.* **1980**, *9*, 91−124.
(23) Catti, M.; Ferraris, G.; Filhol, A. *Acta Crystallogr.* **1977**, *B33*, 1223−1229.

short O−H bonds at 145 K.[24] However, in this study it has not been possible to determine if such H ordering occurs at low temperatures due to the low resolution of the neutron data.

An important feature of the $RbMnHP_3O_{10}$ structure is that channels lie parallel to the [110] and [010] directions (Figures 2 and 3). These channels contain the H^+ sites which suggest that these ions might be exchangeable. However, the failure of attempts to ion exchange H^+ for Li^+ indicates that the very strong hydrogen bonding between triphosphate groups may be necessary to maintain the framework structure. This seems to preclude the possibility of $RbMnHP_3O_{10}$ being a "switchable framework".

The sharp Néel transition observed in the susceptibility data collected from $RbMnHP_3O_{10}$ and the negative Weiss constant, Θ, indicate that three-dimensional antiferromagnetic order occurs below 10 K and the magnetic structure obtained from the low-temperature neutron data is in accordance with this. The magnetic superexchange interactions between spins are mediated by Mn−O−P−O−Mn linkages as the Mn ions are too distant from each other for direct interactions to be significant. Each Mn spin is connected to six others, four in the *bc* plane via Mn−O(2)−P(1)−O(4)−Mn′ bridges, which are apparently ferromagnetic, and two in the [101] direction through antiferromagnetic Mn−O(5)−P(2)−O(5′)−Mn′ linkages. Overall, this corresponds to a primitive tetragonal interaction network giving rise to nonfrustrated antiferromagnetic order. The refined magnetic moment of 3.82(6) μ_B close to the theoretical value of 4 μ_B for high-spin Mn^{3+}. The moments lie in the *ac* plane, in the direction of the long Mn − O bonds (Figure 2), showing that the easy axis is determined by the local electronic anisotropy of the Jahn−Teller distorted MnO_6 octahedra.

In conclusion, through the use of powder diffraction methods, we have determined the nuclear and magnetic structures of $RbMnHP_3O_{10}$, which enable the magnetic susceptibility data and ion exchange inactivity to be explained. Although this material appears not to possess a "switchable framework", it does indicate that a wide range of structures and properties are possible in these $M^IM^{III}HP_3O_{10}$ phases.

Acknowledgment. We thank Dr P. Radaelli for assistance in the collection of neutron data, the EPSRC for provision of neutron facilities and Grant GR/K75040, and the IRC in Superconductivity for access to the SQUID magnetometer.

IC980212L

(24) Catti, M.; Ferraris, G.; Mason, S. A. *Acta Crystallogr.* **1980**, *B36*, 254−259.